

A COMPARISON OF THEORETICAL AND ACTUAL
BEAM PERFORMANCE OF A 140 MEV ELECTRON
LINEAR ACCELERATOR AT THE UNIVERSITY OF SASKATCHEWAN

J. Haimson
Varian Associates
Palo Alto, California

and

L. Katz
University of Saskatchewan
Saskatoon, Canada

Summary

The electron beam optics of the injector and microwave system of a two klystron, four-section linear accelerator with an unloaded beam energy of 140 MeV are discussed. The injector contains a microwave chopper, a nanosecond inflector and a prebunching assembly so that a wide variety of different injection conditions can be presented to the machine. The waveguide sections are of non-uniform impedance design and each is energized by 8.5 megawatts peak r-f power. The design parameters of the waveguide sections are discussed together with the electron beam dynamics for various modes of injector operation, and some comparisons are made with measurements of the electron beam characteristics.

Introduction

Until recently, few scientists outside of the laboratories who pioneered the design, construction and use of linear electron accelerators, appreciated the merits and versatility of these machines for research in nuclear physics and related fields.

The development of reliable high power klystrons and increased sophistication in the state-of-the-art of accelerator manufacture over the past four years has resulted in reliable high intensity machines. The following paper describes an accelerator designed and constructed by Varian Associates for the University of Saskatchewan and gives some of the performance characteristics of the completed machine.

It may be in order to add a word of explanation for the original choice of parameters. Obviously the basic limitation was imposed by the funds available; this however still afforded considerable room for a wide choice of variables. In effect the funds determined the power of the facility and to some extent the degree of sophistication, especially when this involved stepping outside the manufacturers previous experience.

An attempt was made to satisfy a number of experimental needs to make the facility truly versatile.¹ The duty cycle of the machine could not be varied very much without adding a considerable R and D expenditure; on the other hand, short duration pulses and improved repetition

rates were technically feasible. The decision was thus made to aim for 5 ns pulses at 1400 pps. For neutron time-of-flight work, the neutron flux is nearly linearly dependent on the beam power with some advantage to higher beam energy. The higher energy, and resulting lower beam current, commensurate with cost, was thus advisable. In particular, the higher energy and resulting higher momentum transfer in elastic and inelastic electron scatter experiments was a much desired characteristic. Taking all these factors into consideration led to the final choice of the machine characteristics outlined below.

Accelerator Parameters

The performance specifications of the accelerator and pertinent design parameters are listed in Table I.

Table I

Specification

Loaded Beam Energy at 158 mA	98 MeV
Unloaded Beam Energy	130 MeV
Peak Beam Current at 90 MeV	158 mA
Peak Beam Current at 10 MeV	40 mA
Beam Pulse Length	.01 to 1.0 μ s
Energy Spread at 50% Integrated Current	5 MeV

At 624 Pulses Per Second

Beam Pulse Length	1.0 μ s
R-F Flat Top	1.78 μ s
Average Beam Current	98 μ A
Average Beam Power	9.6 kW

At 1400 Pulses Per Second

Beam Pulse Length	.01 μ s
R-F Flat Top	0.78 μ s
Frequency	2856 Mc

Design Details

Number of Klystrons (Type TV-2011-B)	2
Peak R-F Power per Klystron	18 MW
Average R-F Power per Klystron	20 kW
Number of Accelerator Sections	4
Accelerator Section Input Coupler	
R-F Power (Design Value)	8.55 MW

Accelerator Section No. 1

Length	3.36 meter
Number of Cavities	96
Total Voltage Attenuation	0.43 Neper
Filling Time	0.62 μ s
Unloaded Beam Energy	26.7 MeV
Loaded Beam Energy at 158 mA	22.0 MeV
Loaded Beam Energy at 270 mA	18.7 MeV

Accelerator Sections 2 through 4

Length	5.04 meter
Number of Cavities	144
Total Voltage Attenuation	0.57 Neper
Filling Time	0.81 μ s
Unloaded Beam Energy	37.9 MeV
Loaded Beam Energy at 158 mA	28.6 MeV

Total Unloaded Beam Energy	140.4 MeV
Total Beam Energy at 158 mA	107.8 MeV
Computed Energy Spread (50%)	
Integrated Current at 158 mA)	2.0 MeV
Beam Diameter 90% Current, above 15 MeV	1.0 cm

Accelerator Waveguide Section No. 1

This section was designed with a high initial electric field in order to satisfy the capture and bunching requirements of injected electrons in the 90 to 120 keV range. A total attenuation parameter of 0.43 neper and an overall length of 3.36 meters to achieve an unloaded beam energy of 26.7 MeV required an impedance distribution which varied over wide limits. A phase-velocity-of-light structure of $2\pi/3$ mode was used throughout with an initial field strength of 167 kV per cm at 8.55 megawatts peak input power. The zero beam loading electric field strength falls to 149 kV per cm over the first four wavelengths and thereafter is reduced fairly rapidly to 56 kV per cm towards the center of the guide before increasing again to 73 kV per cm at the output. Uniform impedance circuits interconnected by transition sections were used to obtain this distribution. In the interest of minimizing angular momentum, both the input and output couplers were of symmetric field design with iris dimensions of 0.7920 inches and 0.9650 inches respectively. The maximum group velocity, occurring over the central section of the waveguide, is 0.0315 c and corresponds to an iris aperture of 1.1180 inches.

A comprehensive phase orbit analysis was conducted using an improved computer program which more accurately monitors the power flow and electric field vector orientation due to beam loading and non-synchronous trajectories through variable impedance circuits. The waveguide performance was studied for a wide variety of injection conditions which included d-c injection, prebuncher, chopper/prebuncher combination and chopper alone. Figure 1 shows the computed energy and phase distribution from the first waveguide section for various injection potentials and two conditions of beam loading, over a range of injection phase angles. Although velocity modulation content of the injected beam is not a major contributing factor to

energy spread from the first waveguide section, especially for restricted input phase width of say $\pm 20^\circ$ as can be produced with chopper techniques, the broadening of the emergent bunch phase width due to this modulation contributes to energy spread during traversal of the subsequently located waveguide sections. A notable feature of the improved computer program was the indication of small but consistently larger emergent bunch widths with increasing beam loading, than obtained from the original program.

Information from Figure 1 and similar surveys have been used as the basis of a two-stage Monte Carlo program for determining energy spectra characteristics from the machine. This program superimposes upon the ideal machine performance, a series of random and known fluctuations of the system parameters which include electric field amplitude and phase, frequency, injector parameters and system temperature. The initial distribution of charge within the bunch is divided into a series of elements which are followed throughout the length of the machine in a three-dimensional matrix containing the electron energy, phase position and charge content per element.

Accelerator Waveguide Sections Nos. 2 Through 4

These waveguides were designed for an unloaded beam energy of 37.9 MeV with 8.55 MW of input r-f power, and 28.6 MeV when loaded at 158 mA. The residual r-f power under this loaded condition is slightly in excess of 5 percent of the input power. The sections are 504 cm in length containing 144 cavities and closely approach a constant gradient design of 75 kV/cm (for $i = 0$) with the exception of the last three wavelengths over which the attenuation parameters are relaxed to cause a 5 percent reduction in field strength. The iris aperture varies from 1.1640 inches at the input to 0.9233 inches at the output with corresponding group velocities of 0.0315 c and 0.0136 c respectively. Symmetric field coupling cavities are utilized at both ends of the waveguide having pass-band values of 97 Mc at the input and 40.5 Mc at the output.

All three sections are of identical design and are connected to the first waveguide via a six foot dummy drift space length which can be replaced by a positron converter and magnetic confinement system. Positron operation had not been commenced at the time of preparing this article, but the technique to be adopted has been described elsewhere.^{2,3} A typical waveguide assembly during construction is shown in Figure 2. The sections were matched and tuned consistent with a $\pm 0.1^\circ$ C water temperature control and ± 10 kc frequency variation, i.e. an overall phase accuracy with the high attenuation ($IL = 0.57$) guides of

$$\theta = \left(\frac{0.01}{2856}\right)^2 \cdot 13,000 \cdot 0.57 \cdot 57.3 = 3^\circ.$$

Injection System

The injection system comprises a diode

electron gun with a space charge limited cathode emission of 4 Amperes at 105 kV, an r-f transverse magnetic chopper cavity, an electrostatic inflector system for short pulse operation, a prebuncher cavity, tungsten collimators and steering and focussing coils. The gun is pulsed by a separate line type modulator which operates into a resistive load in parallel with the electron source. The indirectly heated carburized thoriated tungsten cathode is temperature regulated by a feedback controlled bombarder system. The beam, in converging from a 14 mm diameter at the entry plane of the gun anode to a 3 mm diameter 13 cm from this plane, passes through an adjacently located chopper cavity and thin magnetic lens assembly. The beam diverges from this first minimum position for 17 cm and is then refocussed by a second thin lens after passing through the prebuncher, onto a tungsten clipping aperture located 34 cm from the first beam minimum position. This symmetric arrangement ensures imaging of the beam minimum at the clipping aperture and the first thin lens provides adjustment to compensate for movement of the beam minimum when changing operation from space charge to temperature limited emission. A third thin lens refocusses the beam through a final 2.5 mm injection aperture at the end of the prebuncher drift space. A thin valve is located between the prebuncher and the third lens assembly to allow replacement of components without losing vacuum in the accelerator proper. An insertable beam collimator is also located at this position. By d-c magnetically biasing the beam to one side of the centerline, r-f chopper operation with approximately 2 kW peak input power causes sufficient sweeping of the beam at the tungsten clipping aperture to provide 180° chopped injection per r-f cycle. By suitably phasing the chopper and prebuncher cavities with respect to the accelerator phase, correct prebunching action provides 30° injection with negligible inter-bunch base current.⁴ Two sets of deflection plates are located in the drift region between the chopper and prebuncher cavities. One of each set of plates is grounded and a biasing magnetic field is applied across the second pair of plates. The remaining plate of each set is coaxially driven by a high voltage switch tube to provide independent fast start and stop control of the injected beam. The tungsten collimator, located immediately after the prebuncher, provides clipping action for both the inflector and the chopper and the components are oriented with respect to one another to allow for beam spiralling in passing through the first two thin lens assemblies. (Approximately 6° between the chopper and the first set of plates and 110° between the first and second set of plates.) Figure 3 is a view of the injection system (gun on the right) showing the two inflector switch tube assemblies and the beginning of the first section. Bunch monitoring measurements, obtained by viewing chopped segments of a rotating beam⁵ have demonstrated injected phase widths of less than 30°. By minimizing the diameter of the final injection aperture and locating it in the pole face of a magnetic assembly which provides a strong axial field along the accelerator waveguide, it has been possible to maintain very small beam diameters of

low angular divergence. With a 2.5 mm input aperture a 25 percent transmission loss is experienced at the 2 Ampere level due to the strong radial and longitudinal space charge forces caused by the combined velocity modulation and third thin lens focussing action. (Critical prebunching is produced at approximately 1 kW peak r-f power to the prebuncher cavity.)

Machine Performance (Initial Tests)

Pulsed Energy Spectrometer

To give the machine operator detailed guidance as to the machine performance, a pulsed magnetic spectrometer is used to present a continuous display of the beam energy spectrum by deflecting one in 128 pulses through slits onto a Faraday cup and associated memoscope. The pulsed magnet is swept so that the complete energy spectrum is traced out every few seconds. A sample of such a spectrum is shown in Figure 4. The unanalyzed pulse and the deflected pulse seen through 1.6 percent slits are shown in one photographic trace, (40 mA/cm, 0.2 μs/cm at 98 MeV) while the energy spectrum is shown on the second trace (2 MeV/cm).

Stability Performance

Ripple on Klystron Cathode Voltage
(1.8 μs pulse at 230 kV) less than ± 0.15%
Accelerator Cooling Water System ± 0.1°C
Gun Voltage Ripple (not yet optimized) better than ± 0.4%

Beam Loading Performance (With Prebuncher Only)

(a) 4 Sections Operating	MeV	Peak Current (mA)
	141	9
	119	80
	98	150
	76	280
Energy spread; ~50% current through 1.6 MeV slits.		
(b) Sections 1 and 2 Operating (3 and 4 detuned by cooling water temperature change)		
	43	160
	25	16
	10	170
The 10 MeV spectrum had ~50% current in 3 MeV.		
(c) Backphasing Sections 3 and 4		
	11	100
Spectrum had ~30% current in 1 MeV.		

The beam cross section in all these measurements was of the order of 8 mm diameter and had a divergence of less than 0.2 mr half angle (measured at 10 MeV and 100 MeV).

Short Pulse Operation

Short pulse operation using a coaxial Faraday cup is illustrated in Figure 5. The upper trace was taken at 2 ns/cm with 100 mA/cm at 70 MeV and the lower trace was taken at 20 ns/cm,

100 mA/cm at the same energy.

Using a scintillation detector and recording individual electrons without energy analysis, the dark current in the $1/2 \mu\text{s}$ preceding an 8 ns pulse and $1/2 \mu\text{s}$ following this pulse was less than 10^{-5} of the current in the pulse.

Acknowledgments

The authors would like to acknowledge the co-operative efforts of the Radiation Division staff of Varian Associates and the Saskatchewan Accelerator Laboratory, University of Saskatchewan throughout the design, manufacture and commissioning stages of this machine.

References

1. Katz, L., Nucl. Inst. and Meth. 11, 14 (1961).
2. Lobb, D. E., "The Generation and Acceleration of Positrons", Saskatchewan Accelerator Laboratory Report, SAL-2, (December 1963).
3. Nunan, C. S., Paper E.6, Particle Accelerator Conference, Washington, D.C. (March 1965).
4. Haimson, J., IRE Trans. Nucl. Sci. 9, 32 (1962)
5. Haimson, J., Paper J.2, Particle Accelerator Conference, Washington, D.C. (March 1965).

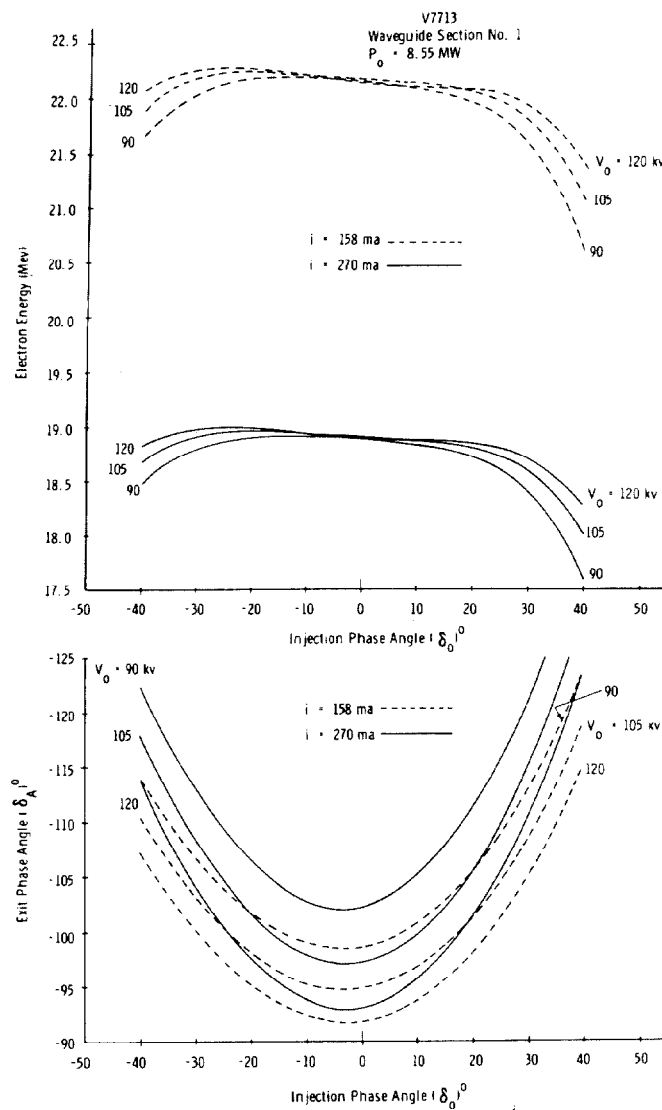


Fig. 1. Beam Design Performance
Waveguide Section No. 1.

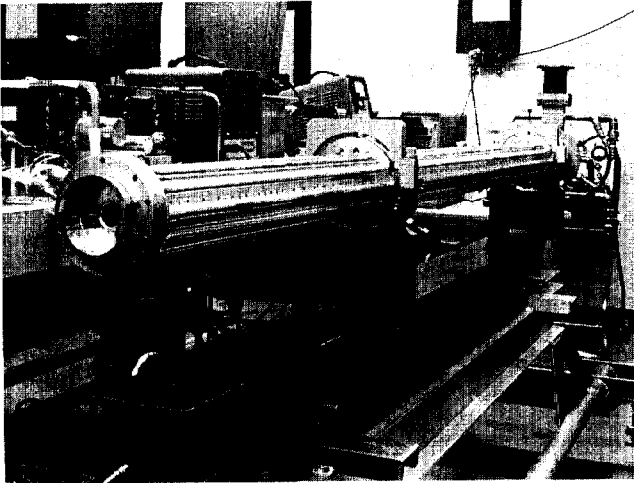


Fig. 2. Typical Waveguide Section during construction.

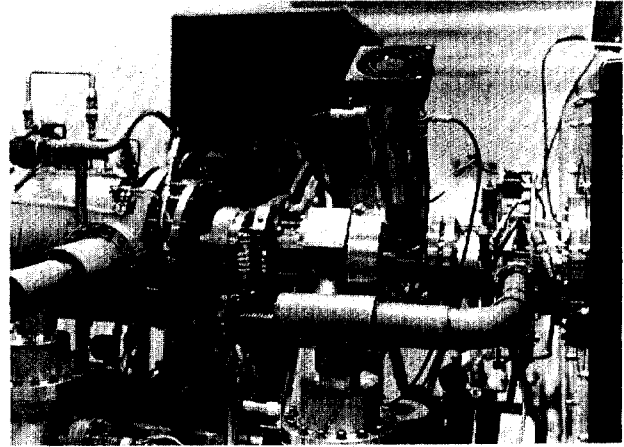


Fig. 3. View of Injection System. The electron gun is on the far right hand side. Electron pulses of the order of $1 \mu\text{s}$ are chopped for $1/6 \text{ ns}$ on and $1/6 \text{ ns}$ off (180° per rf cycle) and then enter the deflection system which selects the duration of the electron pulse presented to the accelerator. The pulses are then bunched so that on inflection into the accelerator they span a 30° phase width of the rf cycle.

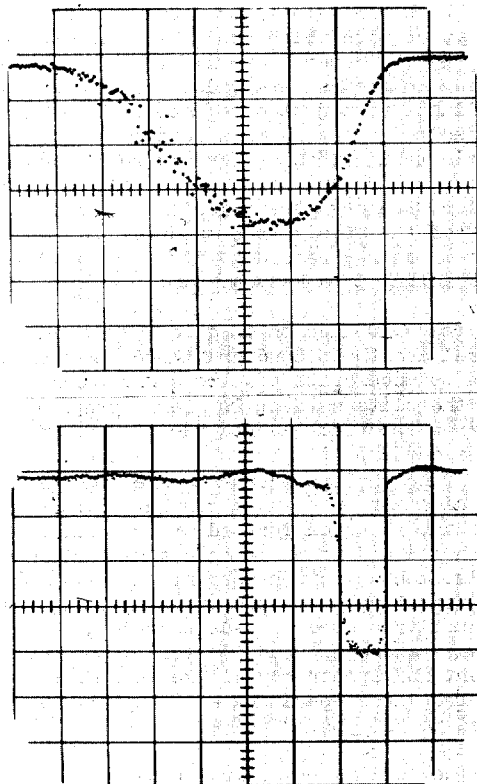


Fig. 4. Upper Trace: unanalyzed electron pulse at the output of the accelerator with a superposed pulse seen through 1.6% energy slits, both pulses swept at $0.2 \mu\text{s}/\text{cm}$ and $40 \text{ mA}/\text{cm}$ sensitivity. Lower Trace: energy spectrum of pulse illustrated above, $2 \text{ MeV}/\text{cm}$.

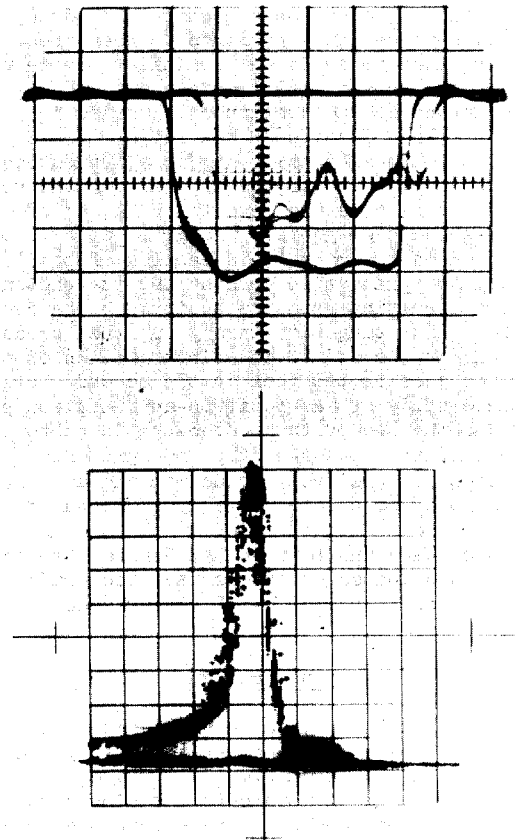


Fig. 5. Upper Trace: fast pulse from accelerator swept at $2 \text{ ns}/\text{cm}$ with $100 \text{ mA}/\text{cm}$ sensitivity at 70 MeV. Lower Trace: 20 ns pulse as seen on a $20 \text{ ns}/\text{cm}$ sweep at $100 \text{ mA}/\text{cm}$ sensitivity.